

April 27, 1995



Office of Nuclear Regulation
U.S. Nuclear Regulatory Commission
Washington, D.C. 20555

Attn: Document Control Desk

Subject: Response to Request for Additional Information
(RAI) Pertaining to the Proposed Technical
Specification Amendment for the Nominal PORV
Pressure Relief Setpoint Versus RCS Temperature
for the Cold Overpressure Protection System

- References:
1. R. Assa letter to D. Farrar dated April 20, 1995, transmitting Request for Additional Information
 2. D. Saccomando letter to the Nuclear Regulatory Commission dated December 16, 1995, transmitting a Proposed Technical Specification Amendment for the Nominal PORV Pressure Relief Setpoint Versus RCS Temperature for the Cold Overpressure Protection System

Reference letter 1 transmitted the Nuclear Regulatory Commission's Request for Additional Information regarding the proposed Technical Specification amendment for the Nominal PORV Pressure Relief Setpoint Versus RCS Temperature for the Cold Overpressure Protection System which was transmitted in Reference 2. Question number 3 mentioned that in Braidwood's submittal, the instrument uncertainties have not been incorporated into the power operated relief valve setpoints for low-temperature overpressure protection curve, and that the Staff found this to be unacceptable. We are enclosing the attached document which summarizes the technical bases for the exclusion of a random instrument uncertainty margin term from the pressure-temperature limits and the cold overpressure mitigation system setpoint. This attachment may be useful during your review to help resolve this issue.

K:\nla\bwd\ltoprai

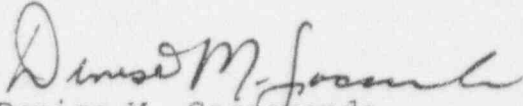
9505020347 950427
PDR ADDCK 05000454
P PDR

ADD 1/1

April 27, 1995

If you have any questions regarding this, please contact this office.

Sincerely,

A handwritten signature in dark ink, appearing to read "Denise M. Sacco". The signature is fluid and cursive, with the first name "Denise" being more prominent.

Denise M. Sacco
Nuclear Licensing Administrator

Attachment

cc: R. Assa, Braidwood Project Manager-NRR
S. Dupont, Senior Resident Inspector-Braidwood
J. Martin, Regional Administrator-RIII
Office of Nuclear Safety-IDNS

Date: November 14, 1994

211866

To: K.L. Kofron R. Kerr
G.K. Schwartz D.E. St.Clair
E.A. Broccolo M.E. Lohmann

Subject: Technical Position on Random Instrument Uncertainty for P-T Limits and COMS Setpoints.

Reference: J.N. Chirigos and T.A. Meyer, "Influence of Material Property Variations on the Assessment of Structural Integrity of Nuclear Components," *Journal of Testing and Evaluation*, Vol. 6, No. 5, September 1978, pp. 289-295 (attached).

At the request of M.A. Gorski, Braidwood SEC, the technical bases for the exclusion of a random instrument uncertainty margin term from pressure-temperature (P-T) limits and cold overpressure mitigation system (COMS, also known as low temperature overpressure protection system, LTOP) setpoints have been summarized. Input to this letter was also provided by Russ Tamminga (Consultant), Jim Chynoweth (SMAD), and Steve Goslin (EPRI-NDE).

Introduction

P-T limits and COMS setpoints are established to protect the reactor pressure vessel (RPV) from nonductile failure due to overpressurization. The determination of the P-T limits and COMS setpoints is based on very conservative assumptions and methodologies. Incorporation of a margin term to account for random instrument uncertainty is not required by the applicable regulations and is not necessary in light of the large margins already present in the determination of the P-T limits and COMS setpoints.

Incorporation of a margin term to account for random instrument uncertainty also:

reduces operating flexibility at low temperatures (operating flexibility as a function of the difference at a given temperature between the maximum allowable pressure in accordance with ASME Section XI Appendix G, and the minimum pressure necessary for proper operation of reactor coolant pump seals), and

increases the likelihood of COMS actuation, endangering reactor coolant pump seals at lower temperatures and unnecessarily challenging the reactor coolant system, with no concurrent increase in protection against nonductile failure of the RPV.

Appendix G Conservatism

Random pressure and temperature instrumentation uncertainties are insignificant when compared to the margin terms already included in the ASME Section XI Appendix G methodology for determining P-T limits, which are subsequently used as an input to COMS setpoints. These margin terms include:

- 1) A safety factor of 2 is applied to the membrane stress intensity factor (pressure). For example, a P-T limit for an allowable pressure of 400 PSIG would actually be based on the stress intensity resulting from a pressure of 800 PSIG.
- 2) ASME Section XI Appendix G allows the sum of the pressure stress intensity factor (multiplied by a safety factor of two) and the thermal stress intensity factor to be no higher than the reference stress intensity factor K_{IC} shown in Appendix G Figure G-2210-1 (attached). The K_{IC} value at a given temperature is the lower bound of all available static, dynamic, and crack arrest fracture toughness data, and is identical to the lower bound crack arrest K_{IC} values shown in Section XI Appendix A Figure A-4200-1 (attached). This is considerably more conservative than either the crack initiation toughness, K_{IC} of Appendix A Figure A-4200-1 (which Section XI Appendix E permits for evaluating the effects of actual overpressure events on the operability of an RPV), or the actual fracture toughness of the RPV limiting material, which would be expected to fall above the K_{IC} curve.

- 3) A 2σ margin on mean predicted shift is included in the Regulatory Guide 1.99 Rev. 2 method for determination of a conservative, upper bound value of adjusted reference temperature. For Braidwood Unit 1 at 32 EFPY and a depth of $1/4T$, this results in the addition of 56°F to the adjusted reference temperature used in the calculation of P-T limits; for Braidwood Unit 2 at 16 EFPY and a depth of $1/4T$, this results in the addition of 52.5°F to the adjusted reference temperature.
- 4) Stress intensity factors are calculated on the basis of an assumed flaw in the wall of the RPV with a depth equal to $1/4 T$. The degree of conservatism associated with this requirement can be seen in Appendix E, which permits the use of a 1.0" initiation crack size. This is considerably smaller than $1/4T$, and is consistent with industry experience in performing ISI of RPV beltline regions.

Illustration of Margin - Chirigos and Meyer Reference

Figure 5 of the Reference (attached) illustrates the conservatism typical of P-T limits developed in accordance with Appendix G for a typical PWR at an end-of-life fluence.

At the lower end of the operating temperature range, where the concern for protection against nonductile fracture is highest, Figure 5 shows that a margin of at least 600 PSIG exists above the Appendix G P-T limit if the sum of the actual pressure and thermal stress intensity factors is not allowed to exceed the K_{IC} curve.

Even greater margins exist when more realistic flaw sizes and the estimated available beltline material toughness is taken into account.

Illustration of Margin - Section XI Appendix E

The Appendix E Paragraph E-1200 Acceptance Criteria can be used to illustrate the conservatism of Appendix G specifically for Braidwood Units 1 and 2.

For Braidwood Unit 1, with a 32 EFPY $1/4T$ adjusted reference temperature of 159°F (56°F of which is Reg. Guide 1.99 Rev. 2 margin), the maximum allowable pressure for a pressurized thermal transient occurring at 214°F is 2485 PSIG (the design pressure). The Appendix G steady-state pressure limit at the same temperature is 935 PSIG, a margin of 1550 PSIG.

For Braidwood Unit 2, with a 16 EFPY $1/4T$ adjusted reference temperature of 145°F (52.5°F of which is Reg. Guide 1.99 Rev. 2 margin), the maximum allowable pressure for a pressurized thermal transient occurring at 200°F is 2485 PSIG (the design pressure). The Appendix G steady-state pressure limit at the same temperature is 912 PSIG, a margin of 1573 PSIG.

The random instrument uncertainty of 60 PSIG and 10°F applied in the past to P-T limits is therefore very small when compared with the margin between the Appendix G P-T limits and the Appendix E allowables. For isothermal pressure transients, the margin available from Appendix E is even higher. And accounting for the shift in the curves resulting from the adjusted reference temperature margin would also result in even higher margins.

Illustration of Margin - Section XI Appendix G

The ASME Code explicitly recognized the amount of margin inherent in Section XI Appendix G P-T limits in the 1993 Addenda. With that Addenda, Appendix G paragraph G-2215 incorporated a provision for allowing COMS setpoints to exceed the usual P-T limits by 10% as a standard practice.

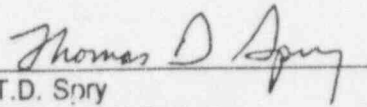
Conclusion

The regulations, Codes, and regulatory positions governing P-T limits and COMS setpoints (10CFR50 Appendix G, ASME Section XI Appendix G, and NUREG 0800 Section 5.3.2 Branch Technical Position MTEB 5-2) do not require margins for random instrument uncertainties.

Compared with the margins inherent in the P-T limits and resulting COMS setpoints developed in accordance with these regulations, random instrument uncertainties are insignificant and additional margin need not be included. Section XI recently recognized this by incorporating a provision for allowing COMS setpoints to exceed Appendix G P-T limits by 10%.

The imposition of margin in addition to that already shown to exist reduces operating flexibility and increases the likelihood of COMS actuation, endangering reactor coolant pump seals and unnecessarily challenging the reactor coolant system, with no concurrent increase in protection against nonductile failure of the RPV.

If there are any questions, please call Tom Spry at 708/663-7268.


T.D. Spry
S/G & RPV Projects

cc: J.C. Blomgren
K. Norris
D. Saccomondo
R.E. Waninski

N.J. Mares
J.M. Chynoweth
H. Pontius

J. Hosmer
R.J. Tamminga
M.A. Gorski

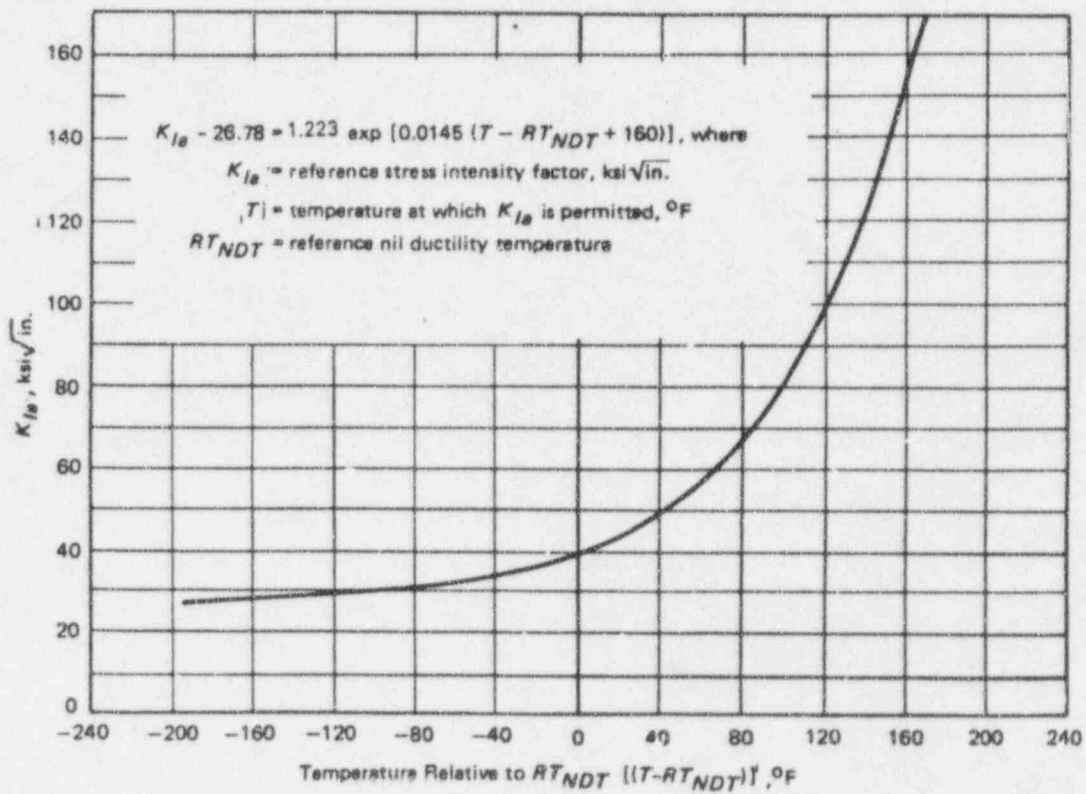
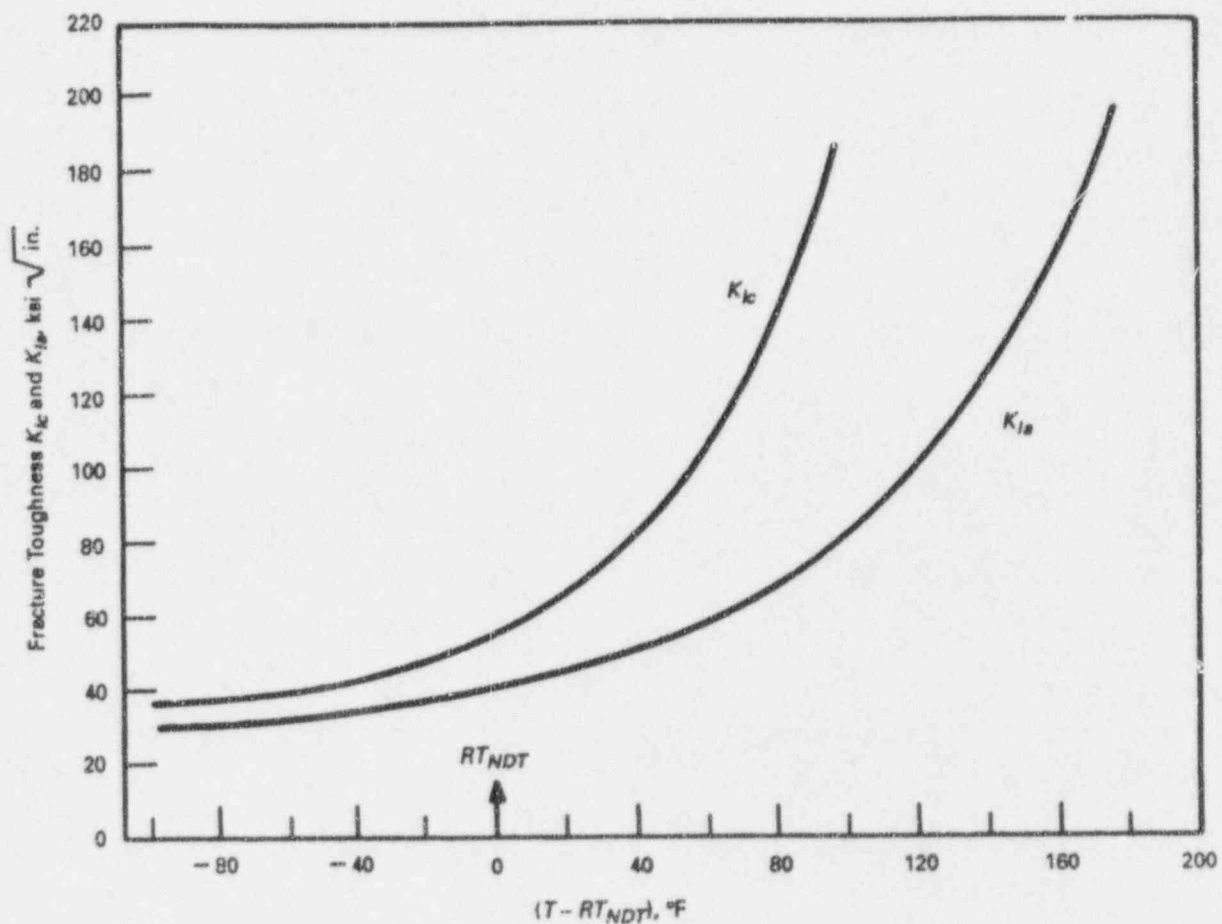


FIG. G-2210-1



A92

FIG. A-4200-1 LOWER BOUND K_{Ic} AND K_{Is} TEST DATA FOR SA-533 GRADE B CLASS 1, SA-508 CLASS 2, AND SA-508 CLASS 3 STEELS

N. Chirigos¹ and T. A. Meyer¹

Influence of Material Property Variations on the Assessment of Structural Integrity of Nuclear Components

REFERENCE: Chirigos, J. N. and Meyer, T. A., "Influence of Material Property Variations on the Assessment of Structural Integrity of Nuclear Components," *Journal of Testing and Evaluation*, JTEVA, Vol. 6, No. 5, Sept. 1978, pp. 289-295.

ABSTRACT: The question, "Where can the generation of new material property data reduce overly conservative design in reactor systems?" presently exists in the nuclear industry. The question is answered by identifying where conservatism exists relative to determining material property variations. Several areas are reviewed to identify conservatism and the sensitivity of structural integrity evaluation results to the property variations. The areas reviewed were fluence dependence of the transition temperature, fracture toughness, the drop in upper shelf toughness, the arrest toughness, the material thermal properties, and the fatigue crack growth rate.

KEY WORDS: nuclear reactors, mechanical properties, fatigue (materials), fracture mechanics, fracture toughness, structural integrity, transition temperature, arrest toughness, fatigue crack growth, nuclear plant heat-up and cool-down, reactor vessel accident analysis, upper shelf toughness

A question presently existing in the nuclear industry is, "Where can the generation of new material property data reduce overly conservative design in reactor systems?" The question can be answered by identifying where conservatism exists relative to determining material property variations in the evaluation of nuclear components' structural integrity and by demonstrating the sensitivity of the structural integrity analysis results to the property variations. The impact of material property variations on the structural integrity of nuclear components can be illustrated by evaluating the structural integrity of a pressurized water reactor vessel. The limiting region of a reactor vessel that should be analyzed in the evaluation of structural integrity is the beltline or core mid-plane region. This region is usually limiting because of the high fluence levels and resulting irradiation damage that occurs in this region.

To assess the reactor vessel integrity it is necessary first to provide a basis for the assessment by considering the applicable standards and criteria used to design, evaluate, and operate a nuclear plant. Then, with these standards and criteria as guides, the evaluation of the sensitivity of the reactor vessel structural integrity to various material property assumptions can be made. This sensitivity is assessed in this report for two sets of plant conditions: those nuclear plant reactor conditions that are con-

sidered normal and are expected to occur and those that are more severe but are not expected to occur (accident conditions).

Applicable Standards and Criteria

The various applicable standards and criteria are these:

- (1) American Society of Mechanical Engineers (ASME) Boiler and Pressure Vessel Code, Section III, Appendix G, "Protection Against Non-Ductile Failure," 1974;
- (2) Code of Federal Regulations, Title 10, Part 50, Appendix G;
- (3) Code of Federal Regulations, Title 10, Part 50, Appendix H;
- (4) ASME Boiler and Pressure Vessel Code, Section XI, 1974;
- (5) ASME Boiler and Pressure Vessel Code, Section XI, Appendix A, "Evaluation of Flaw Indications," 1974;
- (6) U.S. Nuclear Regulatory Commission (NRC) Standard Plan for Pressure-Temperature Operating Limits; and
- (7) NRC Regulatory Guide 1.99, Revision 1, "Effects of Residual Elements on Predicted Radiation Damage to Reactor Vessel Materials," 1977.

The ASME-III, Appendix G, standard presents criteria and methods for prevention of nonductile failure in nuclear components. All loading conditions expected to occur, including normal operation, upset, and test conditions, must be considered. Loading conditions not expected to occur are classed as "accident conditions" and are not considered in the ASME-III, Appendix G, analysis. Appendix G of 10 CFR 50 presents fracture toughness requirements and makes the ASME-III, Appendix G analysis mandatory. Again the conditions classed as "accident conditions" are excluded. Appendix H of 10 CFR 50 requires that the reactor vessel have a surveillance program if the end-of-life fluence is expected to be greater than 10^{17} n/cm² and gives the requirements for such a program.

The ASME-XI standard gives code requirements for in-service inspection, and Appendix A of Section XI requires that defects revealed during inspection be evaluated for accident loading conditions as well as for fatigue. The NRC standard review plan presents guidelines for the NRC reviewer of pressure-temperature operating limits and invokes 10 CFR 50, Appendix G, on all plants, old as well as new, and also requires demonstration of the adequacy of the plant under accident (thermal shock) conditions. The various regulatory guides give suggestions as to how to account for different effects. For example, R.G. 1.99 gives guidance on how to account for the embrittling effects of neutron irradiation.

¹Manager and engineer, respectively, Westinghouse Electric Corporation, P.O. Box 355, Penn Center Building 2, Pittsburgh, Pa. 15230.

Normal Condition Plant Operation

The standards and criteria applicable during normal plant operation are Appendixes G of both ASME-III and 10 CFR 50. The principal material property of interest is the material fracture toughness, which is given in the code as the K_{IR} curve in ASME-III, Appendix G, and as equations for initiation toughness K_{II} and arrest toughness K_{IA} in Appendix A of ASME-XI. The K_{IA} of ASME-XI corresponds to K_{IR} in ASME-III, Appendix G.

Figure 1 gives a plot of K_{II} and K_{IA} (or K_{IR}) as obtained from the ASME-III, Appendix G. Temperature is plotted relative to the reference transition temperature, RT_{NDT} . The code gives no guidance as to the value of toughness on the upper shelf, which is assumed here to be $220 \text{ MPa} \cdot \text{m}^{1/2}$ ($200 \text{ ksi} \cdot \text{in}^{1/2}$). It is felt that this value is supported by existing data; however, the actual value taken is not too important for the task at hand, which will include an assessment of varying shelf toughness.

Fluence Dependence

An important aspect of identifying the toughness curves to be applied to a given situation is to account for the effect of irradiation. This can be accomplished by employing so-called trend curves that give the change in reference temperature with fluence at given copper and phosphorus levels. Regulatory Guide 1.99 presents such curves, as does Ref 1.

As can be seen by examining these documents, there is a difference in the fluence dependence assumed on property changes. This difference is illustrated in Fig. 2. This figure presents ΔRT_{NDT} ($^{\circ}\text{F}$) as a function of increasing fluence. Two fluence trends are shown in Fig. 2: one curve is ΔRT_{NDT} plotted as a function of the square root ($1/2$ power) of the fluence and the second curve is ΔRT_{NDT} plotted as a function of the cube root ($1/3$ power) of the fluence. The impact of different ΔRT_{NDT} fluence curves on reactor vessel structural integrity can now be assessed.

ASME-III, Appendix G Assessment

The Appendix G assessment involves determining the stress intensity factor owing to the design loading conditions acting on an assumed reference flaw usually taken as one fourth of the wall thickness ($1/4T$) in depth. Appropriate safety factors are applied

to the calculated stress intensity factors and it is required that the stress intensity factors (with the safety factors) be less than the value defined by the K_{IR} curve, that is, the reference fracture toughness.

The specific Appendix G evaluation of heat-up and cool-down in nuclear power plants will be discussed separately in a later section of this paper.

By considering the various design loading conditions such as steady state operation and step load change in power, the stress intensity factor is calculated for each loading condition, the appropriate safety factors are applied, and the resulting stress intensity factor is compared with the K_{IR} curve at the temperature where the particular loading condition occurs. An example of the results of this type of analysis is shown in Fig. 3 for an analysis of the beltline region of a four-loop reactor vessel at end-of-life fluence conditions.

The points plotted in Fig. 3 represent the stress intensity factors calculated for individual loading conditions. The position of the reference toughness curve (K_{IR} curve) has been established by two different methods: Method A, $1/2$ power ΔRT_{NDT} -fluence dependence and Method B, $1/3$ power ΔRT_{NDT} -fluence dependence. Even though there is a significant difference in the K_{IR} curve, for these loading conditions, in this particular example ample margin still remains with the curved portion of the K_{IR} curves.

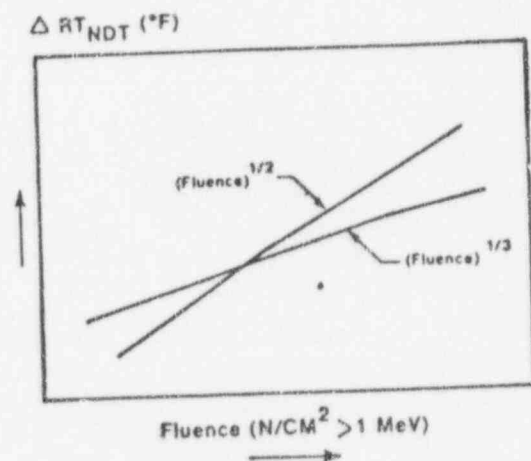


FIG. 2—Change in reference temperature with fluence.

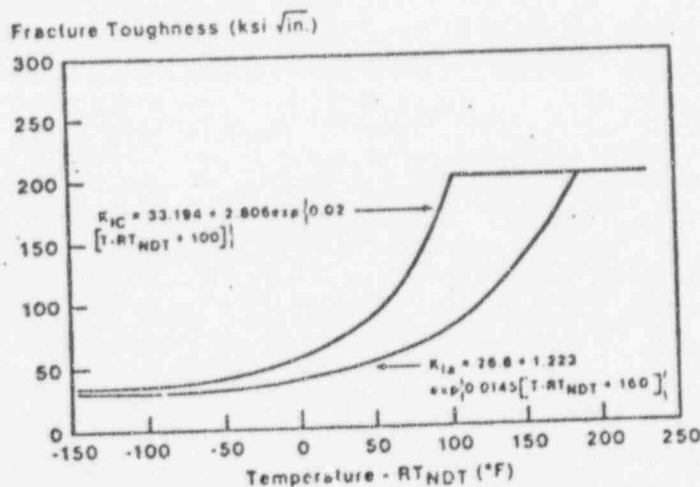


FIG. 1—Reference fracture toughness curves [$1 \text{ ksi} \cdot \text{in}^{1/2} = 1.1 \text{ MPa} \cdot \text{m}^{1/2}$; $^{\circ}\text{C} = (^{\circ}\text{F} - 32)/1.8$].

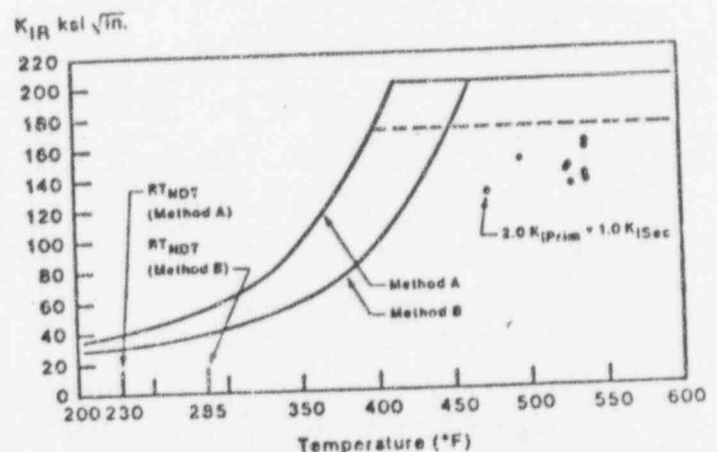


FIG. 3—Temperature curve versus K_{IR} for four-loop reactor vessel at the beltline [$1 \text{ ksi} \cdot \text{in}^{1/2} = 1.1 \text{ MPa} \cdot \text{m}^{1/2}$; $^{\circ}\text{C} = (^{\circ}\text{F} - 32)/1.8$].

There is, however, a less satisfactory situation relative to the proximity of the individual K_I values to the assumed toughness at the shelf. There is ample margin relative to the assumed value of $220 \text{ MPa} \cdot \text{m}^{1/2}$ ($200 \text{ ksi} \cdot \text{in}^{1/2}$) and less, of course, at the value of 182 to $187 \text{ MPa} \cdot \text{m}^{1/2}$ (165 to $170 \text{ ksi} \cdot \text{in}^{1/2}$), which represents the termination of the K_{IR} curve in Appendix G of ASME-III. It should be emphasized that there is considerable conservatism in the calculated stress intensity factors, arising mainly from the factor of 2 on pressure stress intensity and the assumption of a $1/4T$ flaw, as required by ASME-III, Appendix G.

The upper shelf values portrayed in Fig. 3 are considered adequate, in particular for plants built to controlled copper limits. Results from on-going tests will help establish upper shelf levels for older plants with relatively high copper content.

Heat-Up and Cool-Down

Typical heat-up and cool-down limit curves are constructed by the methods of ASME-III, Appendix G, for specified heat-up and cool-down rates, that is, 33°C/h (60°F/h) cool-down rate.

A time period of reactor operation is chosen for which heat-up and cool-down limit curves are to be determined and the RT_{NDT} is then identified. The stress intensity factor K_I for thermal stress is calculated at a specified coolant temperature relative to the RT_{NDT} . The K_{IR} is determined from ASME-III, Appendix G and then the allowable reactor system pressure is calculated which satisfies the relation:

$$K_{IR} > 2K_I \text{ pressure} + K_I \text{ thermal}$$

This procedure is repeated for temperatures covering the range of reactor coolant temperatures of interest and the results are presented as curves of maximum system pressure versus system temperature, as shown in Fig. 4. The curves in Fig. 4 are representative curves for a three-loop, high-copper vessel having an end-of-life fluence.

Two end-of-life limit curves are shown in Fig. 4, one determined by the $1/2$ power fluence dependence, the other by the $1/3$ power fluence dependence of shift in RT_{NDT} . The case chosen was for a

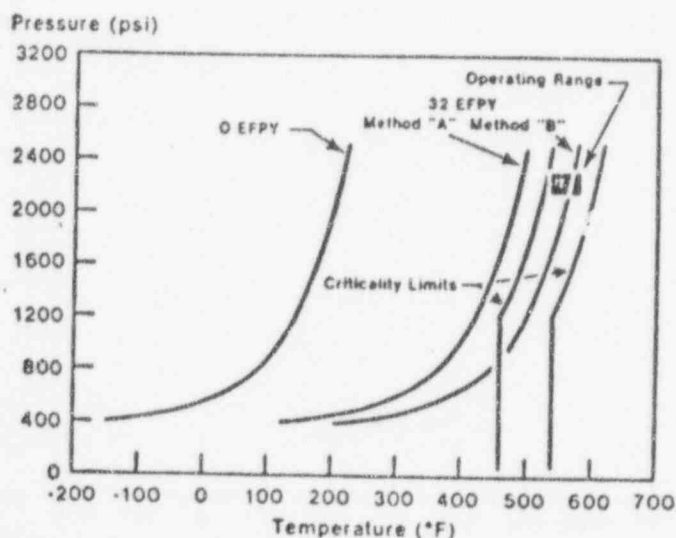


FIG. 4—Operating limits according to ASME-III, Appendix G [1 psi = 6.9 kPa; $^\circ\text{C} = (^\circ\text{F} - 32)/1.8$; EFPP = effective full power years.

reactor design that operates at low average coolant temperature T_{avg} .

The criticality limit is determined by adding a 22°C (40°F) margin to the maximum pressure limit to prevent brittle fracture based on ASME-III, Appendix G. Note that in this case reactor operation is marginal based on Method A ($1/2$ power dependence) and impossible based on Method B ($1/3$ power dependence). Thus, it can be seen that the fluence dependence of ΔRT_{NDT} is a significant parameter that must be established. It is essential that the proper fluence dependence, $1/2$ power versus $1/3$ power fluence dependence, be established since it can determine whether reactor operation is possible at end-of-life conditions, with the assumption, of course, that the margins presently required will be applicable in the future.

It appears that there is a more critical need to establish the effect of fluence on the shift in transition temperature rather than the effect of fluence on upper shelf toughness.

An indication of the conservatism in the ASME-III, Appendix G, limits can be seen in Fig. 5. This figure presents the maximum pressure limit at end-of-life conditions for a three-loop vessel having high (0.30%) copper content.

The lowest curve is that obtained by using the ASME-III, Appendix G, methods. The subsequent curves result by:

- (1) relaxing the factor of 2 on K_I (pressure),
- (2) using the K_{IC} instead of the K_{IR} curve,

Indicated System Pressure (PSIG)

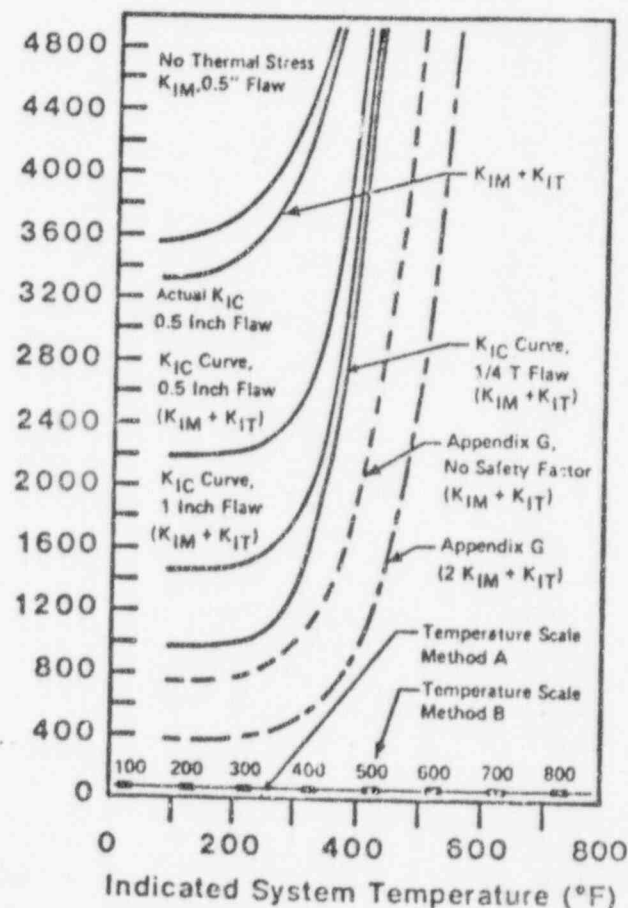


FIG. 5—Reactor vessel cool-down limit curves. $\Delta T/\Delta t$, maximum 33°C/h (60°F/h) [1 psig = 6.9 kPa; 1 in. = 25.4 mm; $^\circ\text{C} = (^\circ\text{F} - 32)/1.8$].

(3) relaxing the assumed critical flaw size from $1/4T$ to 25.4 and 12.7 mm (1 and $1/2$ in.), and, finally,

(4) basing the curve on an assumed "actual toughness," which can be expected to fall above the code K_{IC} curve, a value which may result from the testing of specimens contained in reactor vessel surveillance capsules.

Figure 5 illustrates explicitly the conservatism that exists in the current methods for defining maximum pressure limits. The lower temperature scale results when the toughness curve is shifted by the $1/2$ power fluence dependence as opposed to the upper scale, which is based on the $1/4$ power fluence dependence.

Figure 5 demonstrates the need to establish the correct method of extrapolating the effect of fluence on ΔRT_{NDT} , and it also illustrates the need to assure that shifting the reference toughness curve by use of Charpy data is indeed properly conservative. This can be accomplished by conducting irradiation tests that include both Charpy and fracture mechanics specimens that yield a direct measure of fracture toughness and comparing the shifts in toughness curves. Support for the contention that the method of accounting for the effects of irradiation on toughness using Charpy data to shift the K_{IR} curve is conservative can be seen in Fig. 6.

In Fig. 6 the dynamic fracture toughness obtained from 12.7-mm ($1/2$ -in.) thick wedge-opening-loaded samples irradiated in two different surveillance capsules are plotted. These data, although limited, indicate that the toughness is significantly above the K_{IR} curve, which was positioned by using a $1/2$ power fluence dependence on Charpy data. The dashed curve was drawn with the shape of the K_{IC} curve and positioned by the point at $T - RT_{NDT} = 36^\circ\text{C}$ (100°F). The dashed curve is that used to define "actual" toughness in Fig. 5. This plot also suggests that the shelf toughness for irradiated ($\sim 7 \times 10^{18}$ n/cm²) material is greater than 193 MPa $\cdot\text{m}^{1/2}$ (175 ksi $\cdot\text{in.}^{1/2}$).

Assessment of Vessel Integrity Under Accident Conditions

Accident conditions are those severe conditions which, although not expected to occur, are considered in the reactor vessel design

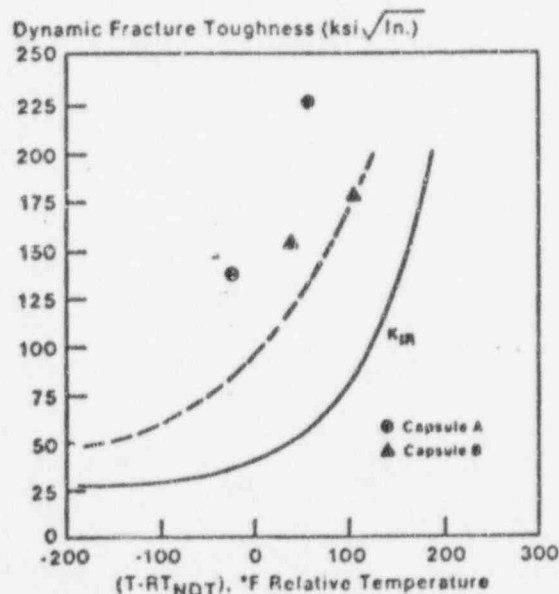


FIG. 6—Surveillance data [$1 \text{ ksi}\cdot\text{in.}^{1/2} = 1.1 \text{ MPa}\cdot\text{m}^{1/2}$; $^\circ\text{C} = (^\circ\text{F} - 32)/1.8$].

because they can produce high thermal stresses in the reactor vessel. To evaluate the reactor vessel under thermal shock conditions [1] a description of the accident transient, usually presented in terms of the coolant pressure and temperature as a function of time into the transient, is first developed. From this information the temperature distribution, or the temperature profile, through the reactor vessel wall at fixed times into the transient is calculated. At a given time into the transient, the temperature profile is used to determine the thermal stress distribution through the wall. The thermal stress and the pressure stress (if any) are then used to determine the stress intensity factors for a postulated flaw of varying depth through the wall. The calculation is usually performed at a given time into reactor life, typically at end-of-life, which provides the maximum fluence at the inside diameter of the vessel. The distribution of fluence through the vessel wall, in conjunction with the temperature profile at a given time into the transient, then permits the determination of the fracture toughness, K_{IC} and K_{IA} , as a function of position in the vessel wall at a given point in vessel life and at the particular time into the transient.

The results of such a calculation can be represented in a plot of stress intensity factor as a function of a/t , where a is the crack depth or position in the wall of thickness t . Such a plot is shown in Fig. 7.

In Fig. 7 the variation of K_I , K_{IC} , and K_{IA} through the vessel wall is presented for 600 s into the transient. Where $K_I \geq K_{IC}$ fracture initiation will occur, and if initiation occurs, arrest will occur when $K_I < K_{IA}$.

It can be seen in Fig. 7 that the K_I curve has just missed the lower part of the K_{IC} curve and that initiation will not occur until some crack depth greater than $0.6 a/t$. Obviously, a slight change in the position of the K_{IC} (or K_I) curve could have lead to initiation at flaw sizes less than $0.1 a/t$.

If similar plots for longer times into the transient are considered, as presented in Fig. 8, it can be seen that the initiation size could be very small or very large depending on how well K_{IC} is

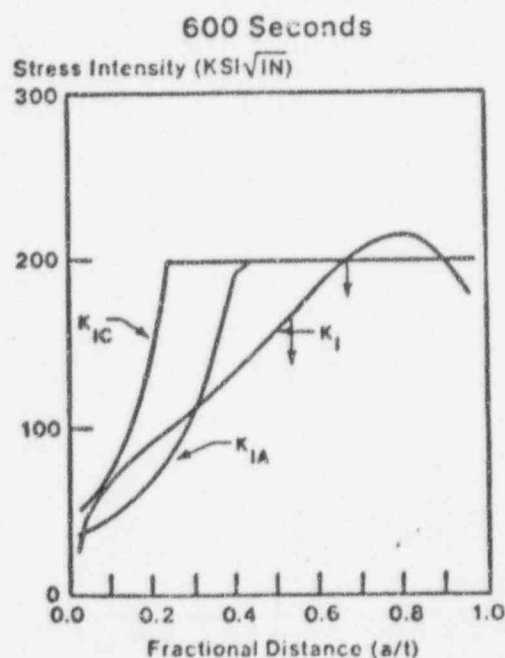


FIG. 7—Thermal shock evaluation for 600 s into the transient [$1 \text{ ksi}\cdot\text{in.}^{1/2} = 1.1 \text{ MPa}\cdot\text{m}^{1/2}$].

known. Actually, in this series of curves, the K_{Ic} value never reaches the K_{Ic} value until the upper shelf, where the critical size (minimum crack initiation depth) is very large in terms of the wall thickness. As illustrated here the results are very sensitive to the location of the toughness curve. Obviously, the method of shifting the unirradiated toughness curves can have a very significant impact on the calculated critical flaw size.

The relationship of the actual vessel toughness to the assumed design K_{Ic} curve can also be very significant in determining the actual critical flaw size determined for the vessel. A small change in toughness can change the intersection point from a very small to a very large value of a/t (or vice versa).

Effect of the Upper Shelf Toughness Value

The sensitivity of the calculated critical flaw size when $K_I > K_{Ic}$ in the upper shelf region is shown in Fig. 9. Here, as before, the standard shelf value has been taken as $220 \text{ MPa}\cdot\text{m}^{1/2}$ (200 ksi-in.^{1/2}), which, for this case, yields a_c (minimum or critical flaw size) of $\sim 0.68 a/t$ —very large. If the shelf were taken as $275 \text{ MPa}\cdot\text{m}^{1/2}$ (250 ksi-in.^{1/2}) there would be no a_c value, which for all practical purposes is not much different than $0.68 a/t$. If the shelf were $182 \text{ MPa}\cdot\text{m}^{1/2}$ (165 ksi-in.^{1/2}), there is, of course, a reduction in the a_c value to $0.54 a/t$, again, very large.

Thus in the case of an accident evaluation the exact value of the upper shelf is not very significant. The opposite is true for the lower portion of the K_{Ic} curve.

Figure 9 also illustrates that if initiation had occurred at about $0.08 a/t$, arrest could be expected at $a/t \sim 0.30$, that is, where K_I falls below the K_{Ic} curve. Thus, the validity of the arrest concept and the location of the arrest curve can be extremely important, in particular when the initiation flaw size turns out to be small.

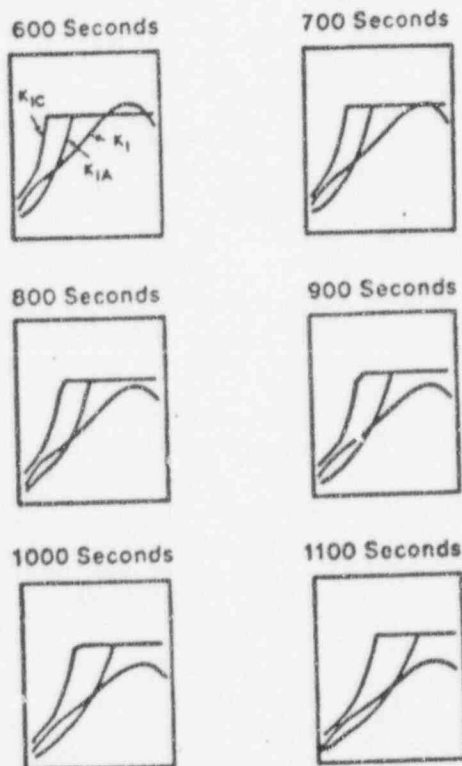


FIG. 8—Thermal shock evaluation for longer times into the transient.

Effect of Thermal Properties

We have, to this point, focused attention on the uncertainties in the critical flaw size calculation that result from uncertainties in the material property values: initiation toughness, arrest toughness, and upper shelf toughness. We have not considered uncertainties in the K_I curve that may result from uncertainties in material thermal properties. Also, uncertainties in material thermal properties can result in changes in the location of the toughness curves since the thermal properties can change the temperature profiles.

In Fig. 10 a temperature profile that results from an assumed reduction of 25% in thermal conductivity, because of irradiation, is compared with the base case, that is, no reduction in thermal conductivity.

It is known that neutron irradiation will reduce electrical conductivity in metals and it is reasonable to assume a reduction in thermal conductivity. To the best of the authors' knowledge the thermal properties of irradiated reactor vessel steel have not been measured. The 25% reduction is arbitrary and was chosen to illustrate an effect.

Very little change occurs in the temperature distribution near the vessel inside diameter, but towards the vessel outside diameter there is about a 28°C (50°F) difference in temperature.

In arriving at this plot, a 25% reduction in conductivity of both clad and base metal was assumed. Other calculations show that the effect of the clad is negligible and the results portrayed are due almost completely to the assumed reduction in base metal conductivity.

The thermal stress profile resulting from this temperature profile is shown in Fig. 11. In this figure it can be seen that a significant increase in thermal stress has resulted from the 25% reduction in conductivity, increased tensile stress in the inner region, and increased compressive stress in the outer region. A fracture

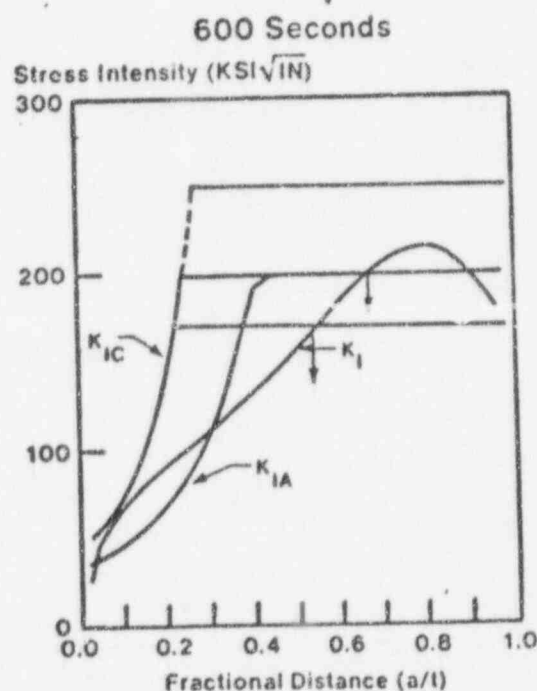


FIG. 9—Thermal shock evaluation; effect of upper shelf ($1 \text{ ksi-in.}^{1/2} = 1.1 \text{ MPa}\cdot\text{m}^{1/2}$).

mechanics analysis would be required to evaluate the impact of changes in thermal conductivity on the reactor vessel integrity.

Fatigue Crack Growth

Data obtained to date for reactor vessel steels indicate a large dependence of crack growth rate on loading frequency and

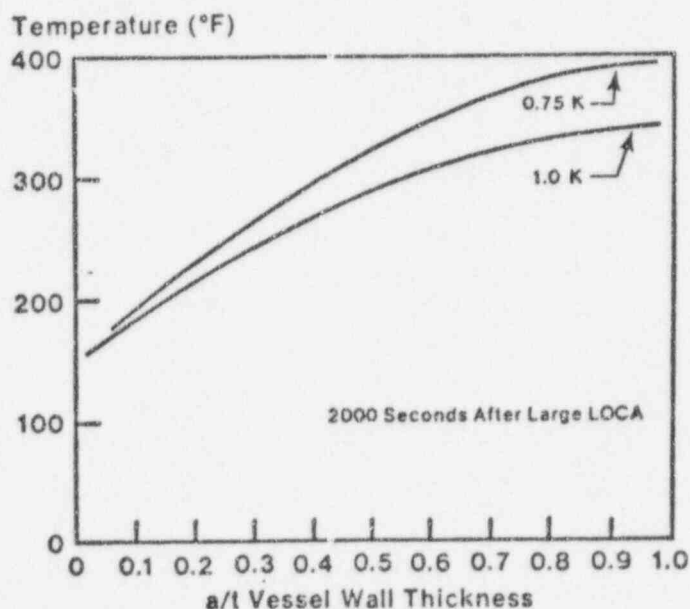


FIG. 10—Temperature profiles: effect of thermal conductivity [$^{\circ}\text{C} = (^{\circ}\text{F} - 32)/1.8$; LOCA = loss-of-coolant accident].

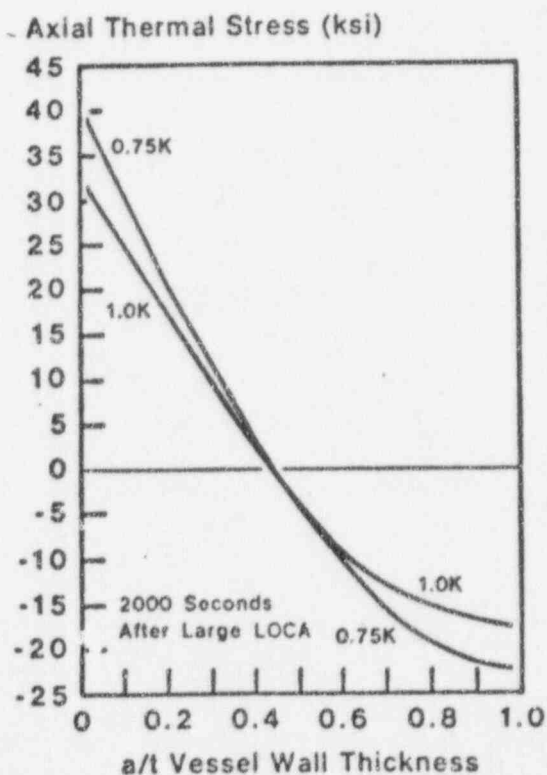


FIG. 11—Thermal stress profiles: effect of thermal conductivity ($1 \text{ ksi} = 6.9 \text{ MPa}$; LOCA = loss-of-coolant accident).

environment—water versus air [2]. At low frequencies the data appear to differ by a factor of about 20 owing to environment, as shown in Fig. 12. This figure is schematic and is intended only to illustrate the difference caused by the environmental effect and the large conservatism contained in fatigue calculations when no consideration is given to the presence of the cladding, which prevents access of the water to the base metal.

The presence of an environmental effect suggests the possibility of an in-pile effect since the radiation environment can break down the water and lead to species which may control the enhanced crack growth rates observed when tests are conducted in water. This is an area that should be evaluated.

There is a dearth of data on crack growth rates pertinent to actual reactor vessel evaluations, that is, irradiated material tested in a water environment. Limited data exist for irradiated material tested in air [3,4] and no data exist for testing in a water environment. There does not appear to be an effect of irradiation on crack growth rates when the testing is performed in an air environment.

Since the present analytical methods, which do not consider the presence of the clad, are conservative for reactor vessel fatigue crack growth evaluations, the analysis results could be improved by obtaining and using more pertinent fatigue crack growth data obtained in vacuum or air environments.

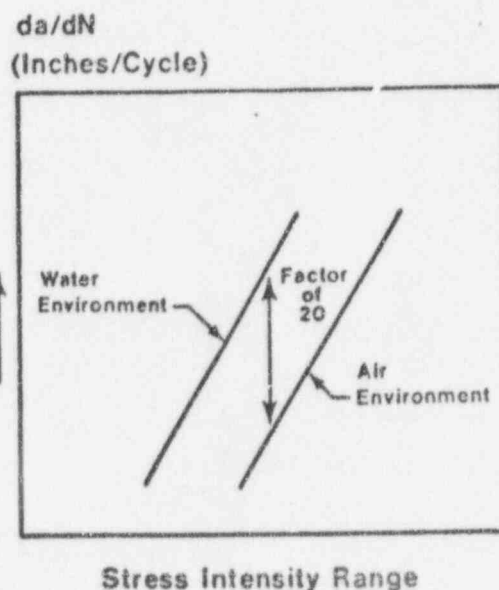


FIG. 12—Schematic diagram of crack growth rate versus stress intensity range ($1 \text{ in.} = 25.4 \text{ mm}$).

Summary

Several areas have been reviewed to identify conservatism in the determination of material property variations and the sensitivity of the structural integrity analysis results to the material property variations. The areas covered were fluence dependence of the transition temperature, fracture toughness and the drop in upper shelf, the arrest toughness, the thermal properties, and the crack growth rate. Major interest is in defining the fluence dependence of irradiation embrittlement, in particular for those evaluations

that require extrapolation into the future with resulting higher fluence. Accurate methods for predicting changes in transition temperature and defining fracture toughness for irradiated material are needed. Indications are that knowledge of toughness in the low toughness region of the fracture toughness curve is more important than toughness at the upper shelf.

When the assessment of a vessel indicates small flaw sizes for initiation and consequent reliance on arrest to demonstrate adequacy, then the arrest toughness for irradiated material must be accurately known.

Finally, the thermal properties of irradiated reactor vessel material should be evaluated since an irradiation effect can affect evaluation of vessel integrity under accident conditions.

As long as cladding is not considered in crack growth evaluation, then the behavior of irradiated material in a water environment must be established, and it should be determined whether an in-pile effect on crack growth rate in a water environment exists. Also, if consideration is to be given for the clad, more crack growth data in vacuum or air should be obtained to eliminate the present conservatism.

Acknowledgments

The authors wish to express their appreciation to J. M. Krampe and O. Meeuwis for their contributions to the technical basis for this paper.

References

- [1] Bamford, W. H. and Buchalet, C. B., "Method for Fracture Mechanics Analysis of Nuclear Reactor Vessels Under Severe Thermal Transients," WCAP-8510, Westinghouse Commercial Atomic Power Division, Westinghouse Electric Co., Pittsburgh, Pa., July 1976.
- [2] Bamford, W. H., Moon, D. M., and Scott, K. V., "Evaluation of Critical Factors in Crack Growth Rate Studies of LWR Steels," presented at the Fourth Water Reactor Safety Information Meeting, Gaithersburg, Md., Oct. 1976.
- [3] Shahinian, P., Watson, H. E., and Hawthorne, J. R., "Fatigue Crack Growth Resistance of Several Neutron Irradiated Pressure Vessel Steels and Welds," *Transactions of the American Society of Mechanical Engineers*, Vol. 96, Series H, 1974, pp. 242-248.
- [4] James, L. A. and Williams, J. A., "The Effect of Temperature and Neutron Irradiation upon the Fatigue Crack Propagation Behavior of ASTM A533B, Class 1 Steel," HEDL-TME-72-132, Hanford Engineering Development Laboratory, Atomic Energy Commission, Washington, D.C., Sept. 1972.